

Supplementary Information

Study of the scale-up, formulation, ageing and ammonia adsorption capacity of MIL-100(Fe), CuBTC and CPO-27(Ni) for use in respiratory protection filters

S. Hindocha^a and S. Poulston^a

Contents

Rietveld refinement fit	1
Nitrogen isotherms.....	6

Rietveld refinement fit

Phase identification was completed using Bruker AXS Diffrac Plus, Eva V19 (1996-2013), Bruker AXS Diffrac Eva V4.0 (2010-2014) software and the ICDD PDF Files: PDF-4+ 2013, COD (REV30738 2011.11.2) database. Crystallite size and lattice parameter measurements were completed using Bruker-AXS Topas 4.2 (1999-2009).

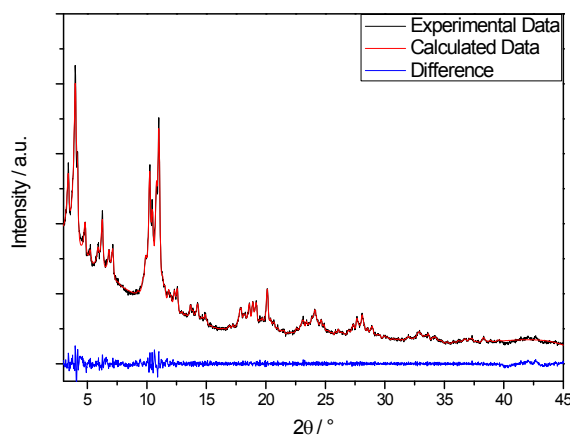


Figure 1. The Rietveld fitting profile of the XRD pattern of MIL-100(Fe) as-synthesised

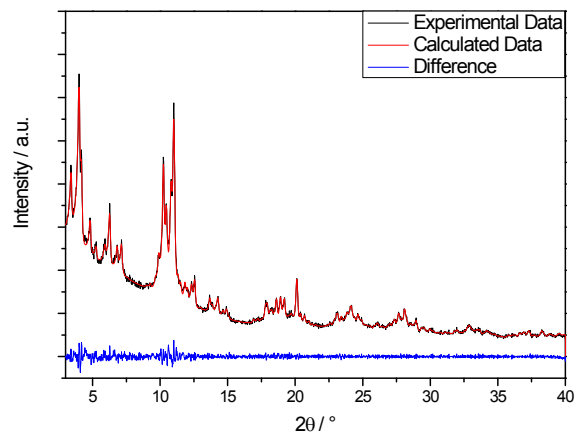


Figure 2. The Rietveld fitting profile of the XRD pattern of MIL-100(Fe)₁

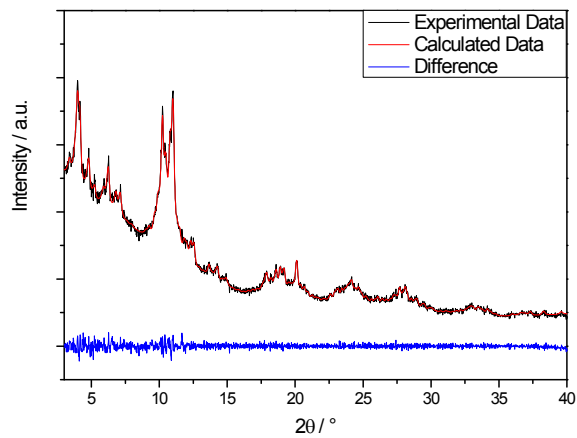


Figure 3. The Rietveld fitting profile of the XRD pattern of MIL-100(Fe)₂

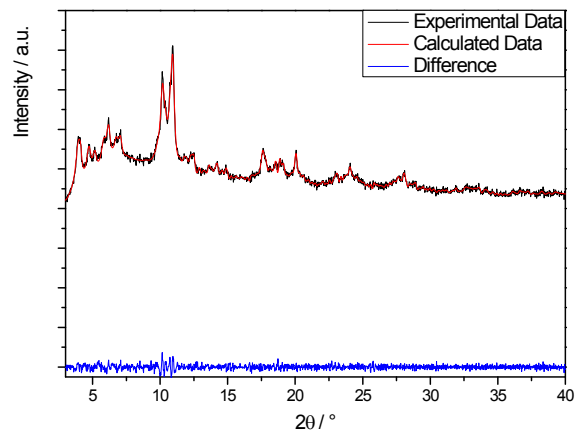


Figure 4. The Rietveld fitting profile of the XRD pattern of MIL-100(Fe)₃

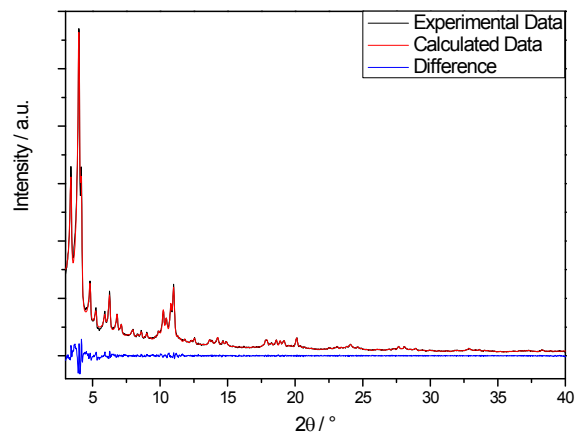


Figure 5. The Rietveld fitting profile of the XRD pattern of MIL-100(Fe)₄

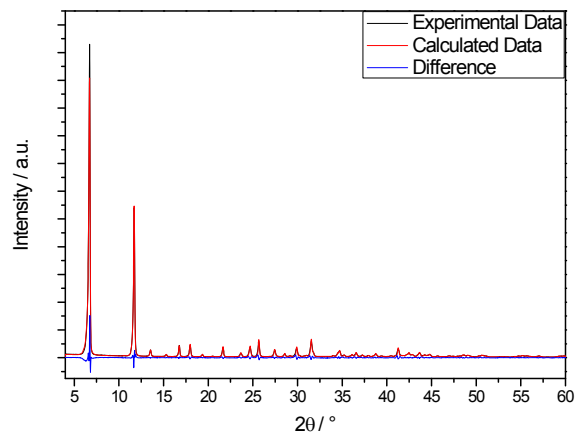


Figure 6. The Rietveld fitting profile of the XRD pattern of CPO-27(Ni) as-synthesised

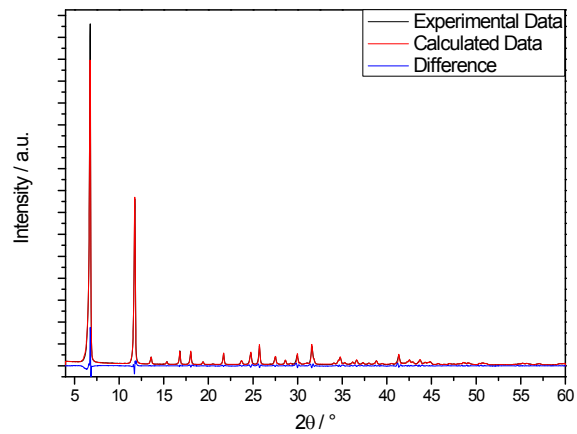


Figure 7. The Rietveld fitting profile of the XRD pattern of CPO-27(Ni)₁

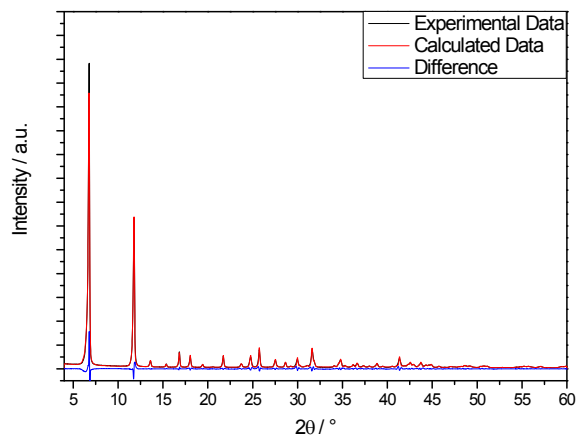


Figure 8. The Rietveld fitting profile of the XRD pattern of CPO-27(Ni)₂

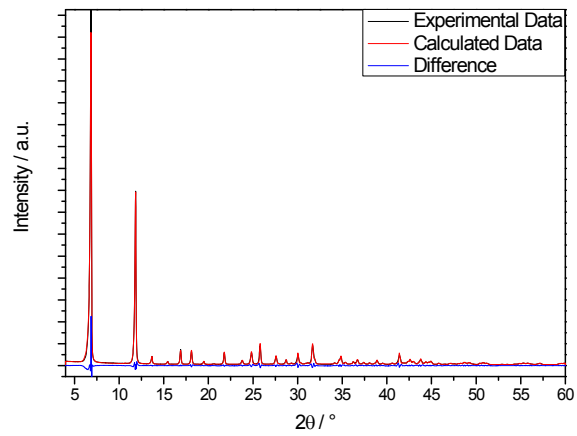


Figure 9. The Rietveld fitting profile of the XRD pattern of CPO-27(Ni)₃

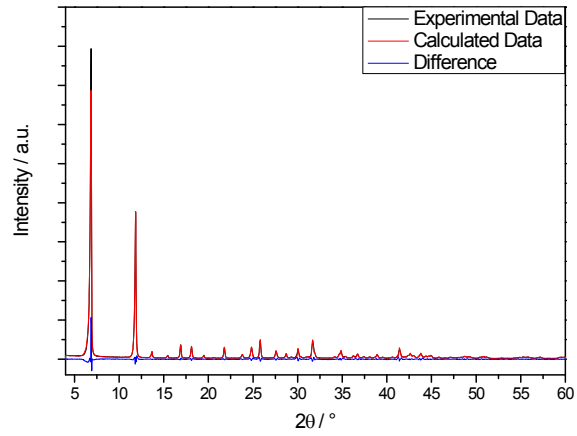


Figure 10. The Rietveld fitting profile of the XRD pattern of CPO-27(Ni)₄

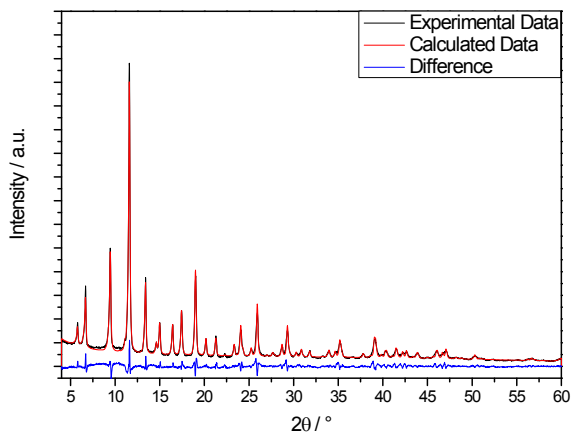


Figure 11. The Rietveld fitting profile of the XRD pattern of Cu-BTC as-synthesised

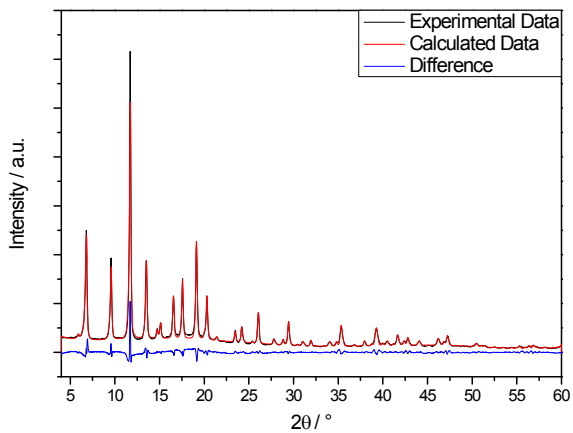


Figure 12. The Rietveld fitting profile of the XRD pattern of Cu-BTC_1

Nitrogen isotherms

Nitrogen isotherm measurements were collected on a Quantachrome Autosorb-iQ-MP at 77 K, 2-station model with each station having 1 Torr, 10 Torr and 1000 Torr transducers. MOF samples were degassed using a two-step programme ramp to 90°C for 2 hours followed by ramp to 150°C for 13 hours. All the BET surface areas were calculated using the Rouquerol method.

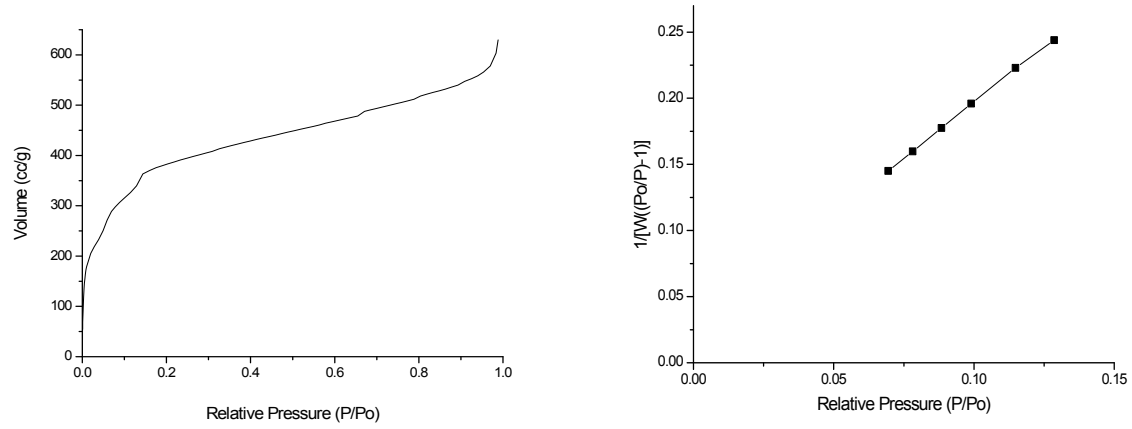


Figure 13. Nitrogen adsorption isotherm and multipoint BET plot for MIL-100(Fe) as-synthesised

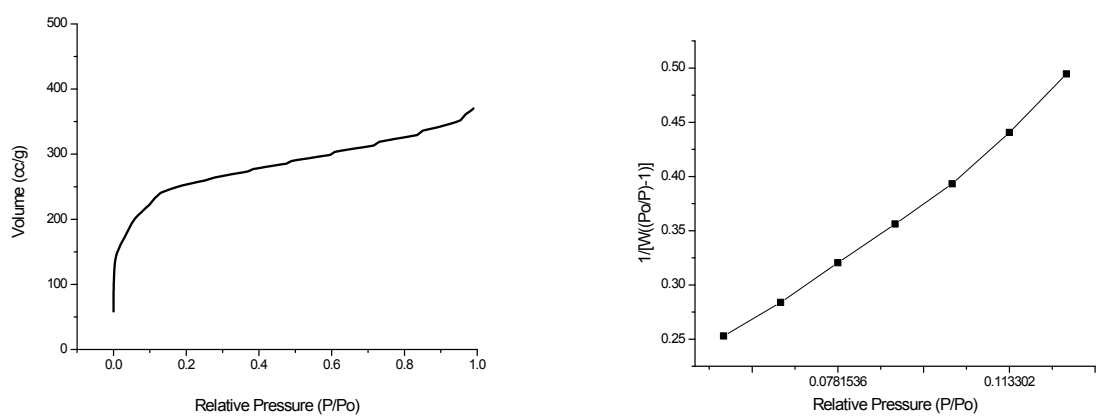


Figure 14. Nitrogen adsorption isotherm and multipoint BET plot for MIL-100(Fe)₁

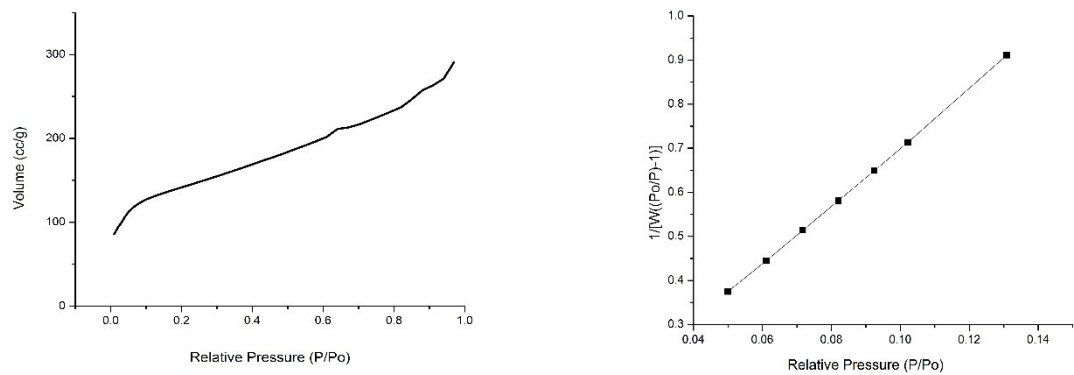


Figure 15. Nitrogen adsorption isotherm and multipoint BET plot for MIL-100(Fe)₂

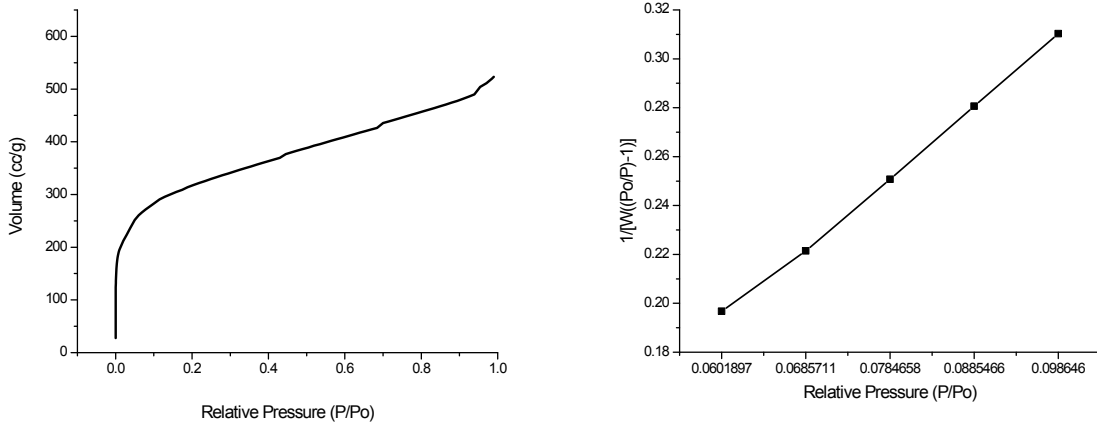


Figure 16. Nitrogen adsorption isotherm and multipoint BET plot for MIL-100(Fe)₃

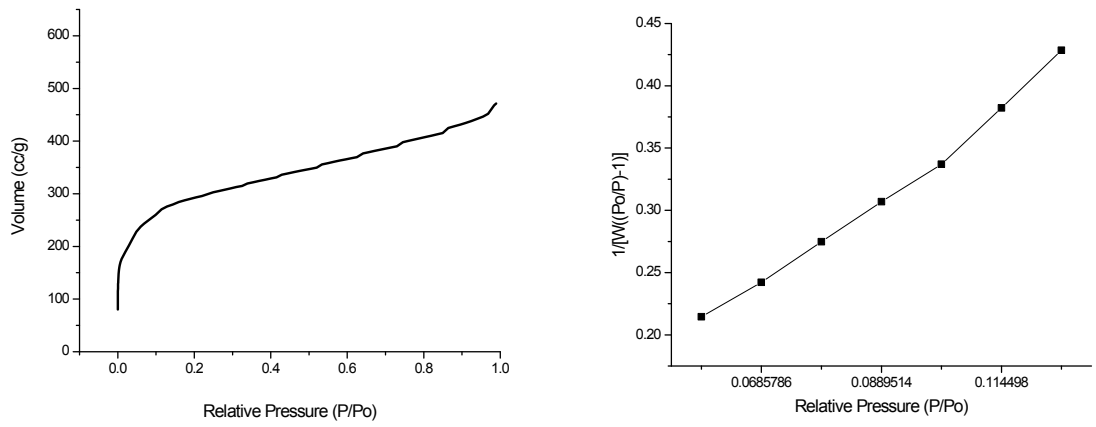


Figure 17. Nitrogen adsorption isotherm and multipoint BET plot for MIL-100(Fe)₄

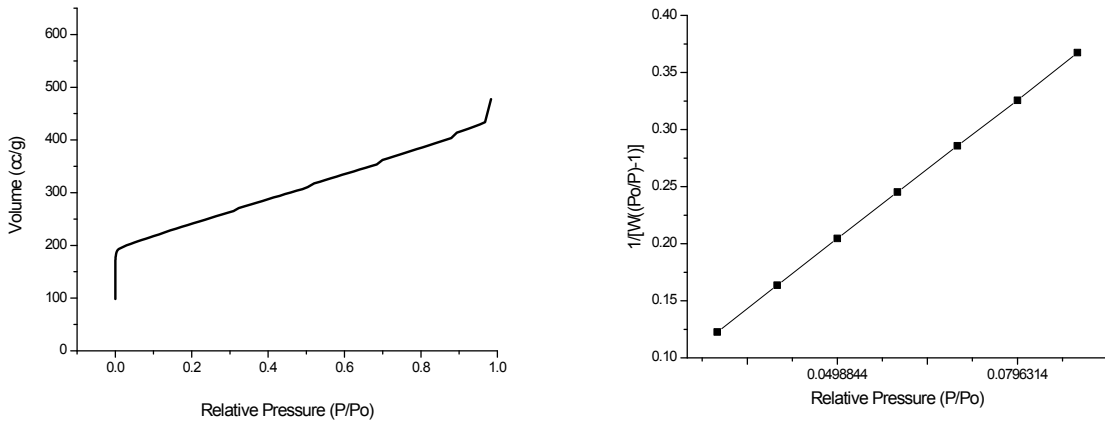


Figure 18. Nitrogen adsorption isotherm and multipoint BET plot for CPO-27(Ni) as-synthesised

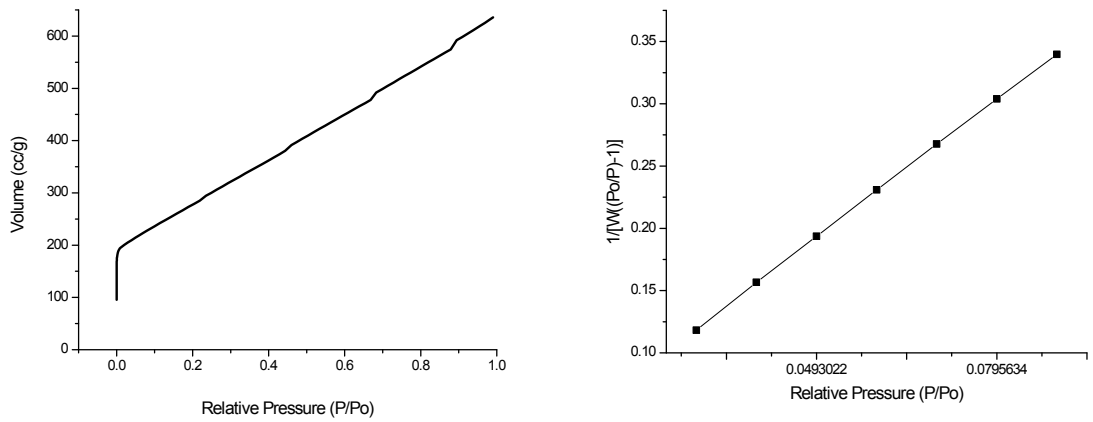


Figure 19. Nitrogen adsorption isotherm and multipoint BET plot for CPO-27(Ni)₁

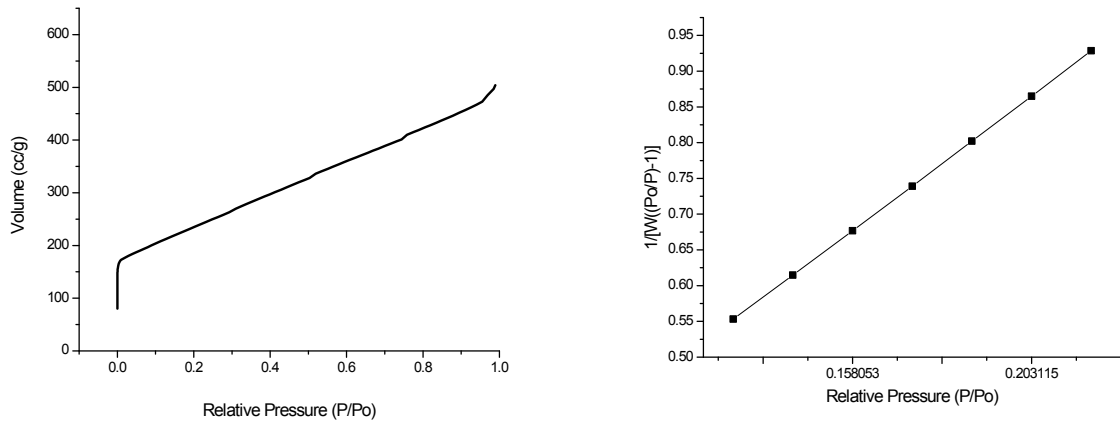


Figure 20. Nitrogen adsorption isotherm and multipoint BET plot for CPO-27(Ni)₂

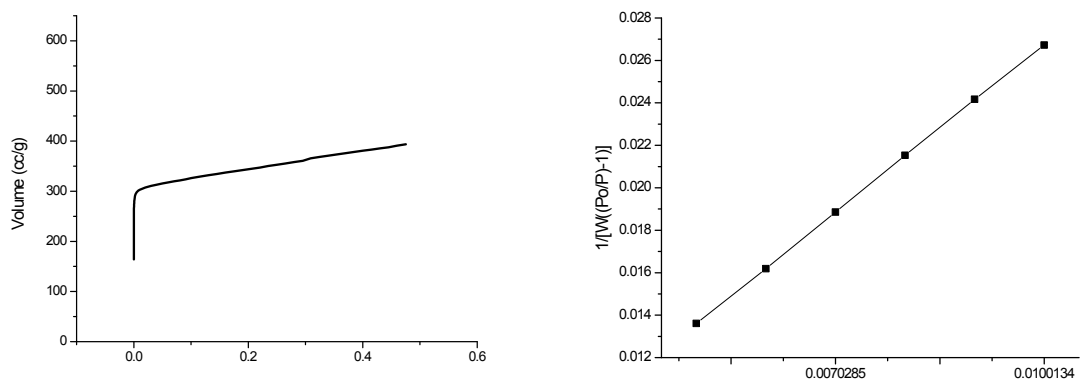


Figure 21. Nitrogen adsorption isotherm and multipoint BET plot for CPO-27(Ni)₃

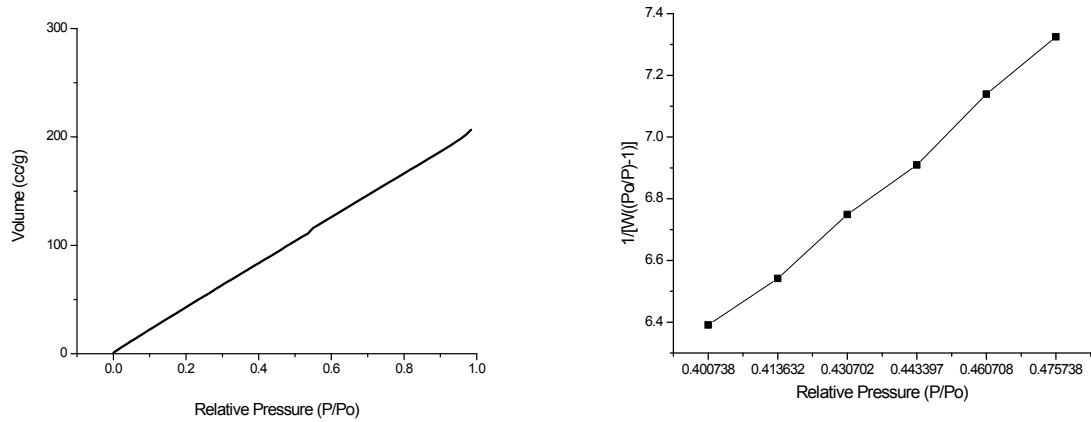


Figure 22. Nitrogen adsorption isotherm and multipoint BET plot for CPO-27(Ni)₄

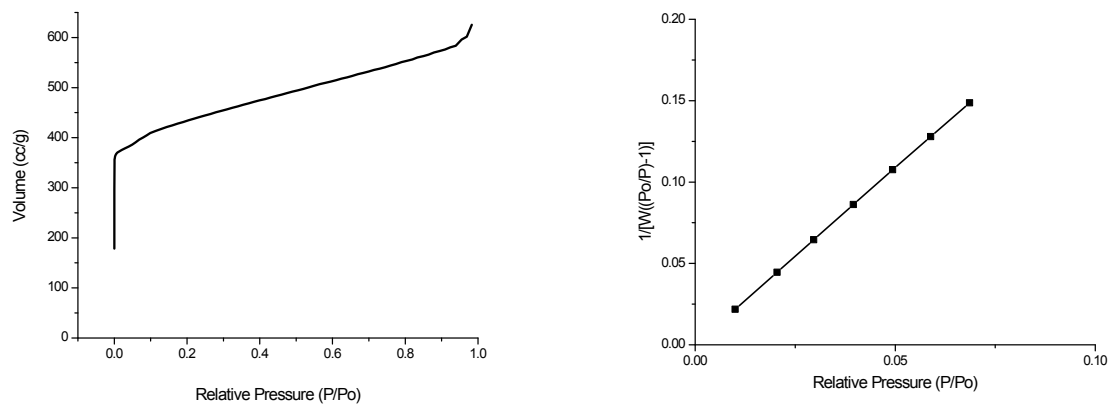


Figure 23. Nitrogen adsorption isotherm and multipoint BET plot for Cu-BTC as-synthesised

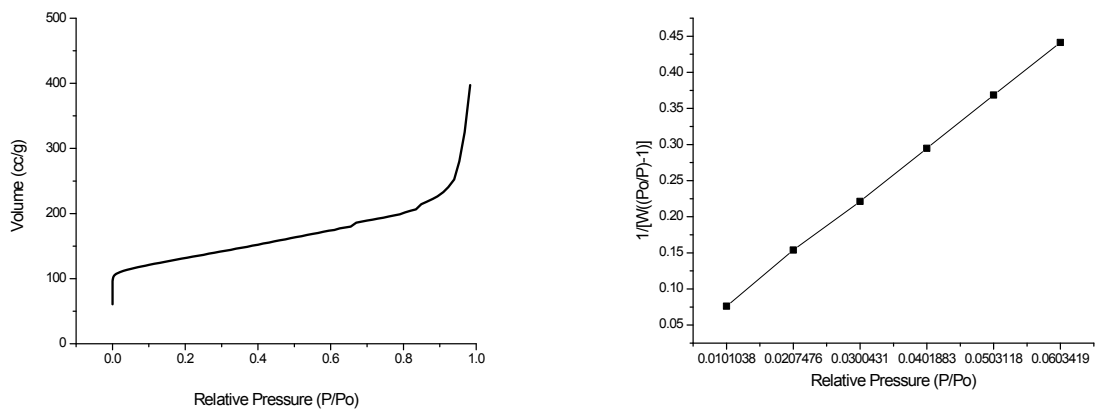


Figure 24. Nitrogen adsorption isotherm and multipoint BET plot for Cu-BTC₁

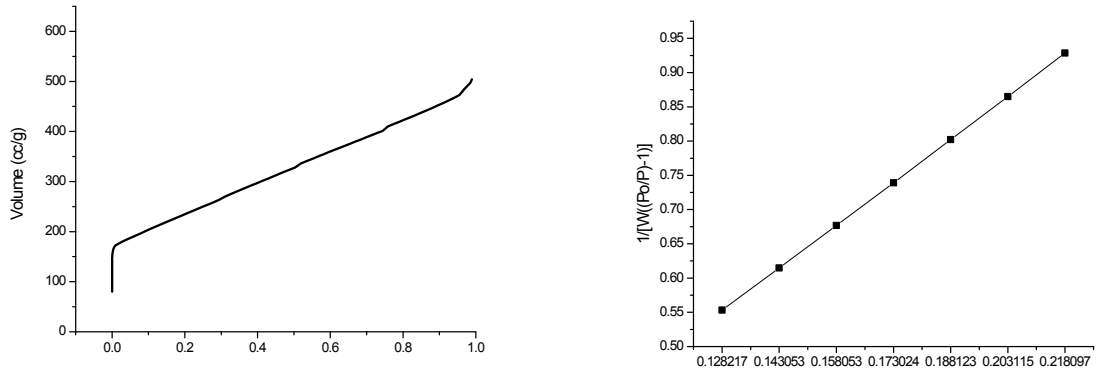


Figure 25. Nitrogen adsorption isotherm and multipoint BET plot for Cu-BTC_2

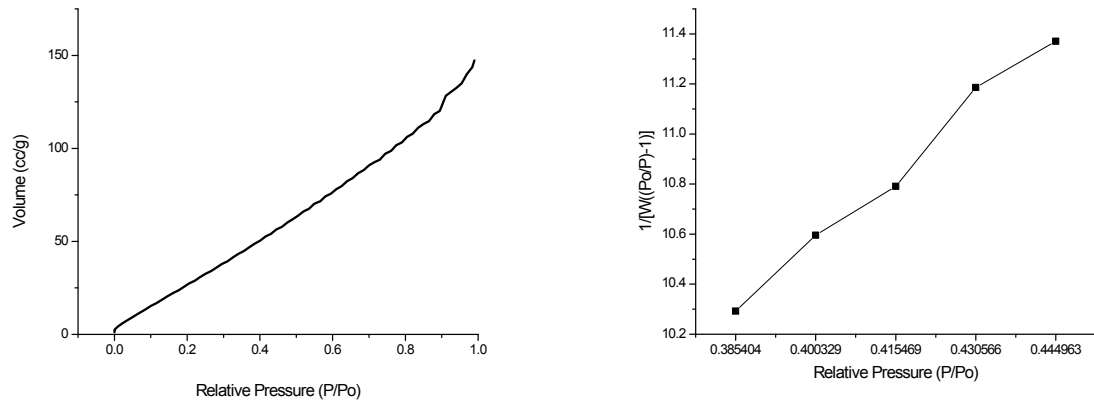


Figure 26. Nitrogen adsorption isotherm and multipoint BET plot for Cu-BTC_3

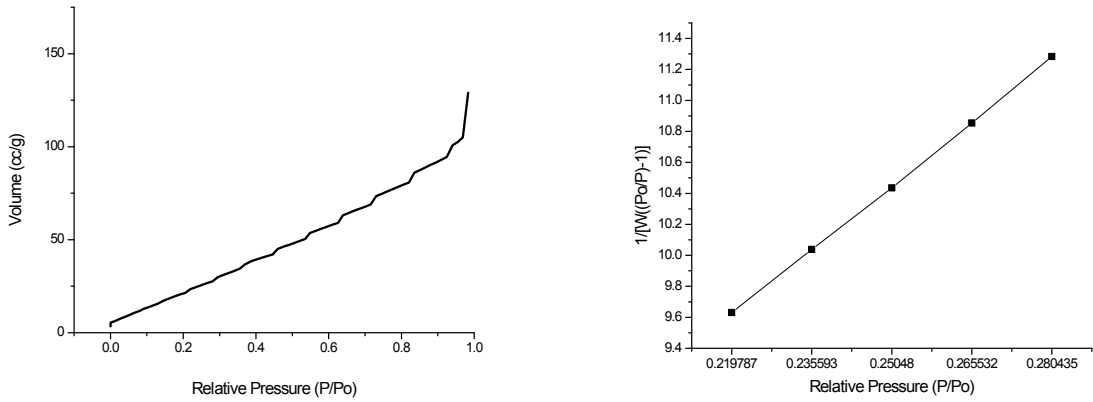


Figure 27. Nitrogen adsorption isotherm and multipoint BET plot for Cu-BTC_4